

# APPLICATION OF MULTIFRACTAL METHODS FOR THE ANALYSIS OF CRYSTAL STRUCTURES

I. Soloviev

St. Petersburg State University  
i.soloviev@spbu.ru

## Abstract

*We discuss here images of complex structure such as biocrystals, which are very often in applications turn out to be fractals or multifractals. We present 3 types of multifractal spectra, and vector characteristics based on blanket technic for the surface of grey-level function constructed by halftone or monochrome image. Such a set of characteristic describes the image structure quite complete. In this work we apply several different fractal and multifractal methods to analyze images. Our experiments make it obvious that for every class of images at least 2 methods allow obtaining reliable separation of numerical signs. The algorithms for calculation multifractal characteristics are implemented. For each class of images the most appropriate signs were recommended.*

## 1. INTRODUCTION

The study of the properties of various biological substances often uses the technique of obtaining their crystalline forms. In medicine, such methods of crystal growth as adding a substance to a solution of copper chloride, as well as adding a medicinal solution to an oil base, are well known.

In many cases, the properties of the substance under study can be judged by the type of crystal obtained. Methods of analysis and classification of digital images play an important role in the study of the properties of biocrystals. For example, in [1, 2] various approaches to the analysis of images of wheat samples are described, including using artificial neural networks.

Very often in applied problems of biology and medicine, researchers work in conditions of the so-called small sample, when the number of samples is in the tens, whereas most machine learning methods rely on the assumption of samples that differ by orders of magnitude. Therefore, mathematical methods for obtaining fine classification features and the use of expert knowledge are of great importance here. Thus, in [3], the method of multifractal analysis was applied to the study of a set of 60 wheat samples. The obtained characteristics combined with expert assessments allowed us to divide the initial set into 5 classes.

The successful application of multifractal characteristics in the analysis of microscopic images of metal sections [4, 5] and in the study of nanostructures [6] shows that the same methods can be used in the analysis of such complex compounds as biocrystals.

The relevance of this research is due to an increasing number of areas in biological and medical research, where the results of experiments can be recorded by obtaining digital images using modern equipment.

In this work, we apply basic methods of fractal and multifractal analysis of digital images to the study of crystals of biological substrates and drugs, which is used in assessing the quality of biological products and laboratory control of drugs.

As classification features in this paper, we use the characteristics obtained by calculating such indicators as the Minkowski dimension, the Renyi spectrum and the multifractal spectrum determined using a local density function, as well as parametrized spectra.

We show that decomposing an image into disjoint level sets using a local density function allows filtering by selecting the set with the largest capacity dimension. Such sets preserve the main features of the original image, and the use of fractal technic allows for a clearer separation of images.

For images of various classes of biological substrates and drugs, we present the results of experiments.

## 2. MAIN DEFINITIONS

### 2.1. Fractal and multifractal characteristics

A natural characteristic of the sets of Euclidean geometry is their topological dimension. It is based on the concept of the multiplicity of the covering

(the smallest number of adjacent elements of the covering  $-1$ , provided that the covering consists of elements having a finite size) and is an integer. Another approach to the notion of dimension was proposed by Hausdorff [7]. For a countable cover with a diameter of elements not exceeding a certain number, we consider a numerical series composed of the diameters of sets raised to a certain power  $p$ . The sum of the series is called the Hausdorff measure, it determines the value of  $p$  at which the series converges. This value, which is not necessarily an integer, is called the Hausdorff dimension. It is known that for sets of Euclidean geometry, this characteristic coincides with the topological dimension. It turned out that the Hausdorff dimension can also be a characteristic for objects of a more complex structure, namely fractals. Such objects are characterized by fractional dimension. According to the definition proposed by the developer of fractal geometry B. Mandelbrot, a fractal is a set for which Hausdorff dimension is strictly greater than its topological dimension.

Fractal sets have the property of self-similarity. This means that the structure of a part of a fractal set is in some way "similar" to the structure of the whole set. Self-similarity can be strict and statistical. The sets for which the law of their construction is known (the Cantor set, the Serpinsky carpet, etc.) of course have strict self-similarity. Most natural objects with a complex structure can be considered as fractals (or multifractals) with statistical self-similarity.

Sets with strict self-similarity are usually constructed iteratively, from a formal point of view, the process of their construction is endless. When depicting such structures, it is believed that the constructed figure approximates the fractal well and gives a visual representation of its shape, if at a certain step of construction the differences become visually imperceptible.

## 2.2. Capacity dimension

In practice, calculating the Hausdorff dimension is a time-consuming task, therefore, the class of so-called "box-counting" (capacity) dimensions is used, which are based on the idea of counting the number of coverage elements of linear size  $\varepsilon$  necessary to cover the set under consideration. When working with fractal sets, we assume that the so-called power law holds, namely, the number of elements of the cover  $N(\varepsilon)$  is proportional to the linear size

of the element in some degree  $N(\varepsilon) \approx c\varepsilon^{-D}$ . This assumption is empirically conditioned.

Usually the capacity dimension of a nonempty bounded set  $F \in \mathbb{R}^n$  is defined as follows

$$D = \lim_{\varepsilon \rightarrow 0} \frac{\ln N(\varepsilon)}{-\ln \varepsilon}.$$

An approximate value of the capacity dimension can be obtained, for example, by using the least squares method.

## 2.3. Minkowski dimension

It should be noted that when analyzing images of fractal sets, the capacity dimension is determined only for black-and-white images.

To calculate the fractal dimension of the sets represented by halftone (gray-scale) images, we can use the Minkowski dimension. It is based on the so-called blanket technic and its calculation does not use a coverage.

A detailed description of this method can be found in [7, 8], so we will provide here only the information necessary to describe the algorithm for its implementation.

Let  $F = \{X_{ij}, i = 0, 1, \dots, K, j = 0, 1, \dots, L\}$  be a gray-scale image and  $X_{ij}$  be the gray level of the  $(i, j)$ -th pixel. This is a gray-level surface for the image, which can be viewed as a fractal for a certain measure range.

Let  $F \subset \mathbb{R}^n$ . Then  $\delta$ -parallel body  $F_\delta$  is a set of points distant from  $F$  by no more than  $\delta$ :

$$F_\delta = \{x \in \mathbb{R}^n : |x - y| \leq \delta, y \in F\}$$

and we say, that  $Vol(F_\delta)$  —  $n$ -dimensional volume of  $F_\delta$ .

If for some constant  $s$  at  $\delta \rightarrow 0$  the limit  $Vol(F_\delta)/\delta^{n-D}$  is positive and bounded, then the number  $D$  is called the Minkowski dimension of the set  $F$ .

We build blankets  $u_\delta, b_\delta$  for a gray level surface as follows

$$\begin{aligned} u_\delta(i, j) &= \\ & \max\{u_{\delta-1}(i, j) + \\ & 1, \max_{|(m,n)-(i,j)| \leq 1} u_{\delta-1}(m, n)\} \\ b_\delta(i, j) &= \\ & \min\{b_{\delta-1}(i, j) - \\ & 1, \min_{|(m,n)-(i,j)| \leq 1} u_{\delta-1}(m, n)\} \end{aligned}$$

$$u_0(i, j) = b_0(i, j) = X_{ij}$$

A point  $F(x, y)$  is included in a  $\delta$ -parallel body if  $b_\delta(i, j) < F(x, y) < u_\delta(i, j)$ . The definition of a blanket is based on the fact that the blanket for a surface of radius  $\delta$  includes all the points of the blanket for a surface of radius  $\delta - 1$  together with the points that are at the distance of 1 from this blanket.

The volume of a  $\delta$ -parallel body is calculated by  $u_\delta$  and  $b_\delta$ :

$$Vol(F_\delta) = \sum_{i,j} (u_\delta(i, j) - b_\delta(i, j)).$$

The surface area is calculated using one of two formulas

$$A_\delta = \frac{Vol_\delta}{2\delta}$$

$$A_\delta = \frac{Vol_\delta - Vol_{\delta-1}}{2}.$$

Minkovsky dimension is defined as

$$D \approx 2 - \frac{\ln A_\delta}{\ln \delta}$$

To obtain the image characteristics, we use a vector  $((\ln \delta, \ln A_\delta))$ , the size of which is determined by the number of different values of  $\delta$ .

## 2.4. Rényi spectra

Consider the set  $M \subset R^n$ , and its partition into  $N(\varepsilon)$  cells with side (or volume)  $\varepsilon$ . We define the probability measure  $p(\varepsilon) = \{p_i(\varepsilon)\}$ ,  $i = 1, \dots, N(\varepsilon)$ ,  $\sum_{i=1}^{N(\varepsilon)} p_i(\varepsilon) = 1$ . Also consider the generalized statistical sum (or the sum of the moments of the measure) [9]

$$S(q, \varepsilon) = \sum_{i=1}^{N(\varepsilon)} p_i^q(\varepsilon), q \in R \quad (1)$$

As usual we assume that the power law holds

$$p_i(\varepsilon) \sim \varepsilon^{\alpha_i} \quad (2)$$

We also assume that the statistical sum itself also follows the power law:

$$S(q, \varepsilon) \sim \varepsilon^{\tau(q)} \quad (3)$$

where  $\tau(q)$  is a function of class  $C^1$ .

The symbol  $\sim$  in (2) and (3) is understood as follows:

$$\alpha_i = \lim_{\varepsilon \rightarrow 0} \frac{\ln p_i(\varepsilon)}{\ln \varepsilon}, \tau(q) = \lim_{\varepsilon \rightarrow 0} \frac{\ln S(q, \varepsilon)}{\ln \varepsilon} \quad (4)$$

Under these assumptions, the characteristic of a set with a complex structure is a set of generalized Rényi dimensions:

$$D_q = \lim_{\varepsilon \rightarrow 0} \frac{1}{q-1} \frac{\ln S(q, \varepsilon)}{\ln \varepsilon} \quad (5)$$

## 2.5. Parameterized spectra

A multifractal set can be represented as a set of fractal subsets, each of which has its own fractal dimension. A multifractal spectrum is a set of dimensions of these subsets. Multifractal spectrum is a set of subsets, each of them is the union of covering elements having close values of exponents  $\alpha_i$  in (4).

In this sense Rényi spectrum is not multifractal one, because it shows the changing of initial measure when parameter  $q$  changes. But one may go from Rényi spectrum to multifractal one by using parametrized spectra [10].

Let  $M$  be a set and  $\{M_i\}$  be its partition on  $N(\varepsilon)$  cells by size  $\varepsilon$ . Consider a normed measure  $\{p_i(\varepsilon)\}$  on  $\{M_i\}$  and construct a sequence of measures  $\mu(q, \varepsilon) = \{\mu_i(q, \varepsilon)\}$ , where

$$\mu_i(q, \varepsilon) = \frac{p_i^q(\varepsilon)}{\sum_{i=1}^{N(\varepsilon)} p_i^q(\varepsilon)}.$$

Define the average  $\alpha(q)$  of exponents  $\alpha_i$  by a chosen measure

$$\alpha(q) = \lim_{\varepsilon \rightarrow 0} \frac{\sum_{i=1}^N \ln p_i(\varepsilon) \mu_i(q, \varepsilon)}{\ln \varepsilon}$$

For every measure  $\mu(q, \varepsilon)$  calculate information dimension  $f(q)$  of its support

$$f(q) = \lim_{\varepsilon \rightarrow 0} \frac{\sum_{i=1}^N \mu_i(q, \varepsilon) \ln \mu_i(q, \varepsilon)}{\ln \varepsilon}$$

Excluding parameter  $q$  we obtain multifractal spectra  $(\alpha, f(\alpha))$ .

### 2.6. Local density function

This method was proposed in [11]. Consider an image  $I$  in  $R^2$  and denote the square with center  $x$  and radius  $r$  (half of the side length) by  $B(x, r)$ . Denote the measure of pixel intensities by  $\mu$ .

Assume that

$$\mu(B(x, r)) = kr^{d(x)}(x), \quad (6)$$

where  $d(x)$  — local density function and  $k$  is a constant.

Consider (6) for  $r$  small enough, then it follows

$$d(x) = \lim_{r \rightarrow 0} \frac{\log \mu(B(x, r))}{\log r}$$

The function  $d(x)$  characterizes the degree of heterogeneity of the pixel intensities distribution in a neighbour of  $x$ . The set of points  $x$  with local density  $\alpha$  forms the level set

$E_\alpha = \{x \in I: d(x) = \alpha\}$ . In practice we calculate  $\alpha_{min}, \alpha_{max}$ ,  $\alpha \in [\alpha_{min}, \alpha_{max}]$  and form the sets

$$E(\alpha, \varepsilon) = \{x \in I: d(x) \in [\alpha, \alpha + \varepsilon]\},$$

where  $\varepsilon$  is a parameter.

We obtain a set of binary images. Obviously, this parameter controls the number of level sets and allows the separation of the image on nonintersecting level sets, and the procedure of separation is a kind of filtration.

Then we calculate capacity dimensions for level sets and obtain multifractal spectrum  $f(\alpha)$ .

## 3. EXPERIMENTS

### 3.1. The effect of cyna

The effect of Cyna 6 on biosubstrates was studied. The images from 2 classes (each contains 5 images) were analyzed by the methods described.

The results are shown below.

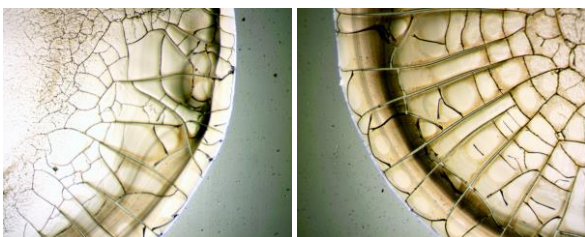


Figure 1. Biosubstrate without correction (left) and after correction (right) .

Graphs are given below. All the calculated features show the separation.

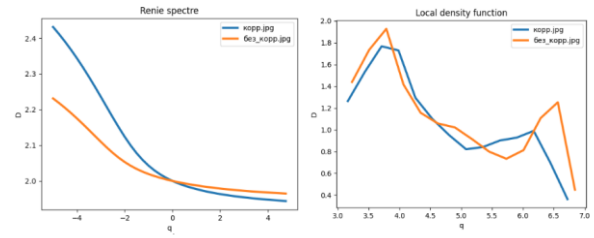


Figure 2. Renyi spectra and multifractal spectra by local density function

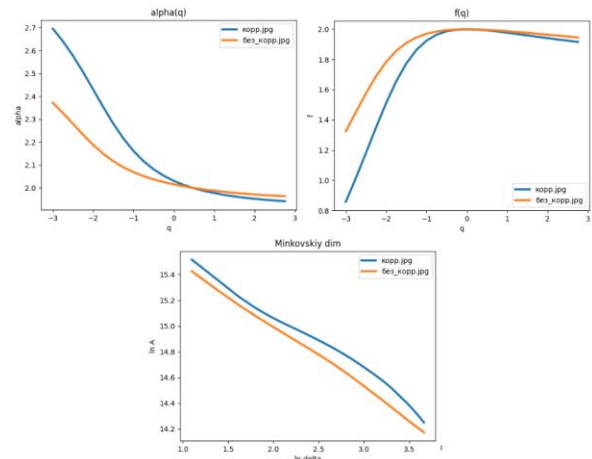


Figure 3. Parametrized spectra and graphs of characteristic vectors

### 3.2. Crystals of drugs

3 types of crystals of drugs (medical solution is added to oil, crystals are formed on the boundary of matters).

Images are obtained by microscope, every class contains 7-8 images.

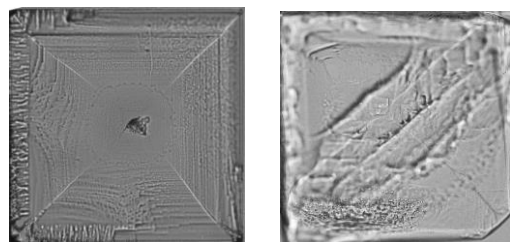


Figure 4. Class 1 (left) and class 2(right)

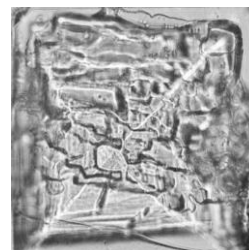


Figure 5. Class 3

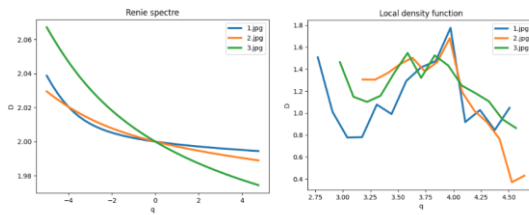


Figure 6. Renyi spectra and multifractal spectra by local density function

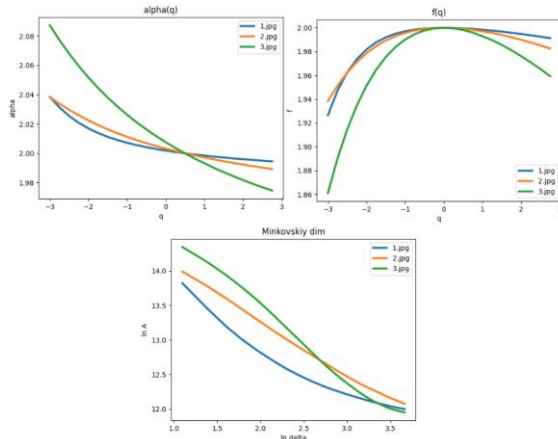


Figure 7. Parametrized spectra and graphs of characteristic vectors

#### 4. CONCLUSION

As a rule, researchers work with images biomedical preparations under conditions of so called small sample — the number of images is estimated in tens, not thousands. It is expert knowledge that has a decisive meaning. However, the practical experience shows that a description of images in terms of numerical characteristics is useful addition to visual perception. Any description of an image structure may be thought as a formalization of expert knowledge. In this work we demonstrate the results of application of several fractal and multifractal methods to analyze images of crystals of drugs. The experiments showed that for every class of images at least 2 methods allow obtaining reliable separation of numerical signs.

#### ACKNOWLEDGMENTS

The author thanks I. Demidov for his significant help in organizing and performing the necessary experiments.

#### References

- [1] Khoshroo A. Classification of Wheat Cultivars Using Image Processing and Artificial Neural Networks / A. Khoshroo, A. Arefi // Agricultural Communications, . — 2014. — № 2 (1). — C.17-22.
- [2] P. Sadeghi-Tehran. DeepCount: In-Field Automatic Quantification of Wheat Spikes Using Simple Linear Iterative Clustering and Deep Convolutional Neural Networks, *Frontiers in Plant Science*. 2019, v. 10. <https://doi.org/10.3389/fpls.2019.01176>.
- [3] Murenin I., Ampilova N. Analysis of Wheat Samples Using the Calculation of Multifractal Spectrum , *Computer Tools in Education*, 2021, № 1,p. 5-20.
- [4] Vstovsky G.V. Elements of information physics M, MGIU 2002. (in Russian)
- [5] Bortnikov A.Y., Minakova N. N. Texturno-fraktalnii analiz mikroskopicheskikh srezov obraztsov rompozitsionnih materialov zapolnennih technicheskim uglerodom, *Izv TPU*, 2006. №6.(in Russian).
- [6] Polischuk S.V., Petrov K.A. Otsenka fraktalnih svoystv nanostruktur po mikroskopicheskim izobrazheniyam, *MNIG*, 2022. №2-1 (116).(in Russian)
- [7] Falconer, K. J. *Fractal geometry* / K. J. Falconer. — Chichester : Wiley,1990.
- [8] Tang, Y. Y. Modified fractal signature (MFS): a new approach to document analysis for automatic knowledge acquisition Y. Tang, C. Y. Suen // *IEEE Transactions on Knowledge and Data Engineering*,1997, 9, № 5,p. 747-762.
- [9] Kuznetsov S.P. *Dynamical chaos*, M, *Izd.fiz-mat lit.*,2001
- [10] Chhabra A. B, Direct determination of the  $f(\alpha)$  singularity spectrum and its application to fully developed turbulence , *Physical Review A*,1989,v. 40, № 9. p. 5284-5294.
- [11] Y. Xu, H. Ji, C. Fermüller , Viewpoint Invariant Texture Description Using Fractal Analysis, *International Journal of Computer Vision*, 2009,v. 83, № 1,p. 85-100.